Effects of Adaptation in Maintaining High Sensitivity over a Wide Range of Backgrounds for *Escherichia coli* Chemotaxis

Bernardo A. Mello*† and Yuhai Tu*
*IBM T. J. Watson Research Center, Yorktown Heights, New York; and †Physics Department, Catholic University of Brasilia, Brasilia, Brazil

ABSTRACT An allosteric model is developed to study the cooperative kinase response of wild-type (wt) *Escherichia coli* cells to the chemoattractant MeAsp in different ambient MeAsp concentrations. The model, together with wt dose response data, reveals the underlying mechanism for *E. coli*'s ability to maintain high sensitivity over a wide range of backgrounds. We find: 1), Adaptation tunes the system to the steepest part of the dose response curve, where the sensitivity to a given type of stimulus is amplified by the number of corresponding receptors in the (mixed) functional receptor complex. A lower bound on the number of Tar receptor dimers (N_a) in the complex $N_a \gtrsim 6$ is obtained from the measured sensitivity. 2), Accurate adaptation synchronizes the kinase activities from different (uncoupled) receptor complexes in a single cell and is crucial in maintaining the high Hill coefficient in the (population averaged) kinase response curve. 3), The wide dynamic range of the high sensitivity can be explained in our model by either having a very small ratio between ligand dissociation constants of the inactive and the active receptors $C = 0.006$, $N_a = 6$, and a (methylation level independent) dissociation constant for the inactive Tar receptor $K = 18.2\ \mu$M or by having K and/or N_a increase with receptor methylation level together with a larger value of $C > 0.01$. Specific experiments are suggested to distinguish these two scenarios. 4), The receptor occupancy in a wt cell should also adapt and exhibit a slow (approximately logarithmic) dependence on the ligand concentration in the adapted state; this general prediction can be tested experimentally to verify/falsify our model.

INTRODUCTION

Despite their diversity in molecular details, biological sensory systems, from chemotaxis in bacteria (1) to vision, olfactory, and hearing in higher organisms (2), share the essential ability of detecting small changes of stimulus in a wide range of ambient backgrounds. Understanding the molecular mechanisms underlying this robust signal detection and amplification process is at the center of studying sensory signal transduction. The advantage of working with sensory system in bacteria is that a molecular level description of how the signal is received, transduced (to the flagellar motor), and regulated has been worked out for bacterial chemotaxis in *E. coli* (for recent reviews, see references (3,4)). In particular, the discovery of chemoreceptor clustering (5) has provided the important structural basis and insight for understanding receptor level signal amplification (6–8) in bacterial chemotaxis. However, despite the qualitative level knowledge of the underlying signaling pathway, many important quantitative questions remain unanswered. For example, the sensitivity, defined as the ratio of fractional changes in receptor kinase activity and that of the ligand concentration, can now be measured quantitatively and found to far exceed that of a system composed of independent receptors (9,10). Furthermore, this heightened sensitivity exists for a wide range of backgrounds, e.g., spanning three to four orders of magnitudes in methyl-aspartate (MeAsp) concentrations (9,11). Understanding the underlying mechanism for these quantitative observation will not only reveal important information about the structure of the receptor cluster and the quantitative effects of adaptation (through receptor methylation) for bacterial chemotaxis, it may also shed light to the study of other more complicated biological sensory systems.

Due to the quantitative nature of the questions mentioned above, computational modeling has emerged as a powerful tool in understanding these complex systems. Recently, there has been a burst of activities on quantitative modeling of bacterial chemotaxis, directly stimulated by a series of in vivo response measurements (9,12) from the Berg lab using florescence resonance energy transfer (FRET) technique. The Ising-type models (13–15), wherein receptors sit on the sites of a regular lattice and interact with their neighbors, were the first proposed to explain these quantitative (FRET) dose response data for both the adaptation-disabled mutants and the wild-type (wt) cells. The quantitative agreement between the experimental data and the Ising-type model (13) confirmed the existence of receptor interaction in general and interactions between different types of chemoreceptors in particular for the first time from the in vivo response data (9). However, the Ising-type models have their limitations, partly due to their inherent complexity, which makes it difficult to determine the properties of the individual receptor and the properties of the receptor cluster from the response data. Most recently, a simpler, more intuitive model for describing receptor cooperativity in bacterial chemotaxis has been developed by several groups (12,16–18), based on the Monod-Wyman-Changeux (MWC) model (19) of allosteric protein interaction. In Sourjik and Berg (12), used the original MWC model to explain the kinase response of the

Submitted October 3, 2006, and accepted for publication December 18, 2006.
Address reprint requests to Yuhai Tu, E-mail: yuhai@us.ibm.com.

0006-3495/07/04/2329/09 $2.00
doi: 10.1529/biophysj.106.097808

adaptation-disabled mutant strains with a single type of major receptors. In our own work (17), the MWC model was generalized to describe kinase activity of a mixed cluster consisting of different types of chemoreceptors and other cytoplasmic proteins (CheW and CheA); this generalized MWC model was used to study signal integration and explain response data for different mutant strains to different stimuli. The resulting parameters were directly related to properties of the individual receptors and the properties of the receptor complex. Keymer et al. (18) examined the general properties of the MWC-type model and found two distinctive types of behaviors in the model that resembles the qualitative behaviors of the response data for receptors with different methylation levels; these general findings were later used to argue in favor of the MWC-type models (20).

In this article, we extend the allosteric model by incorporating effects of adaptation to describe the kinase response in wt cells adapted to different ambient backgrounds. By fitting the in vivo response data (9) for wt cells in different backgrounds quantitatively with our model, we seek to understand the molecular mechanism underlying both the large magnitude and the wide dynamic range of the high sensitivity in wt *E. coli* cells. Specifically, we want to study the properties of the receptor complex, such as the number of receptor dimers it contains, as well as the properties of the individual receptor, e.g., if and how much the receptor's ligand binding affinity depend on its methylation level. More generally, we aim to elucidate the roles of adaptation in bacterial chemotaxis in maintaining the high sensitivity over a wide dynamic range of backgrounds.

METHODS: AN ALLOSTERIC MODEL FOR THE WT CELL

There are five types of chemoreceptors in *E. coli*: two high-abundance ones, Tar and Tsr, and three low-abundance ones, Trg, Tap, and Aer. The chemoreceptors (of all types) together with other relevant cytoplasmic proteins, such as the histidine kinase CheA and the linker molecule CheW can form functional complex. The polar receptor cluster in an *E. coli* cell contains many such complexes. Receptors within a functional complex are tightly coupled and can switch between their active and inactive states in an all-or-none fashion. MeAsp, a chemoattractant, binds to the Tar receptor in the complex with different dissociation constants K or K/C depending on whether the complex is in its inactive or active state. Binding of MeAsp to Tar biases the complex toward being inactive, and Tar in an inactive complex binds stronger with MeAsp, i.e., $C < 1$. These two factors form a positive feedback for the activity and give rise to the cooperative response of the complex. Quantitatively, for a wt *E. coli* cell that has adapted to MeAsp concentration $[L]_0$, after a sudden MeAsp concentration change to a new level $[L] = [L]_0 + \Delta[L]$, the (immediate) kinase activity (A_{wt}) of a functional complex can be expressed by a MWC type allosteric model:

$$A_{wt}([L],[L]_0) = \frac{L\left(1 + C\frac{[L]}{K}\right)^{N_a}}{\left(1 + \frac{[L]}{K}\right)^{N_a} + L\left(1 + C\frac{[L]}{K}\right)^{N_a}}, \quad (1)$$

where N_a is the number of Tar receptor dimers in the functional complex and L is the overall equilibrium constant for the whole complex, corresponding to the relative probability of the complex being in the active state in the absence of ligand. For detailed derivation of the model, see references (17,18). For simplicity, we neglect the distribution of methylation levels for receptors within a functional complex. In addition, in the range of MeAsp concentrations (<10 mM) where experimental data are available, we can also neglect MeAsp binding to Tsr. The validity and possible effects of these two approximations will be discussed in the Discussion section.

Adaptation in bacterial chemotaxis occurs by methylation and demethylation of the chemoreceptors facilitated by the enzymes CheR and phosphorylated CheB, respectively. The parameters (N_a, L, K, and C) in Eq. 1 characterize the properties of the receptor complex and can therefore depend on the receptor methylation level, which in turn depends on the background ligand concentration ($[L]_0$) that the cell adapts to. To study how adaptation affects kinase response in different backgrounds, we need to know how these parameters depend on the background ligand concentration $[L]_0$. This dependence can be obtained by enforcing known experimental observations for the adapted state in our model without explicit modeling of the methylation kinetics. For MeAsp response, the wt cell adapts (near) perfectly (9,21), we thus set the adapted activity to be a $[L]_0$ independent constant $a_0 < 1$ in our model:

$$A_{wt}([L]_0,[L]_0) = a_0,$$

which leads to the explicit dependence of the adapted equilibrium constant L on $[L]_0$ and other model parameters K, C:

$$L = \frac{a_0}{1 - a_0}\left(\frac{K + [L]_0}{K + C[L]_0}\right)^{N_a}. \quad (2)$$

The activity expressed by the MWC model, Eq. 1 with the (perfect) adaptation condition expressed in Eq. 2 constitute the adaptive allosteric model to describe the response of the wt *E. coli* cell to any change in MeAsp concentration $\Delta[L]$ after it adapts to the background MeAsp concentration $[L]_0$. In the following, by analyzing this model and fitting it to the wt response data (9), we aim to understand the underlying mechanism for the cell's high sensitivity and its wide dynamic range.

RESULTS

The high sensitivity and the lower bound on the size of the receptor complex

The most important quantity to characterize the dose response curves is the sensitivity, defined as the ratio between the fractional change in activity $\frac{\Delta A_{wt}}{A_{wt}([L]_0,[L]_0)}$ and the fractional ligand concentration change $\Delta[L]/[L]_0$ as $\Delta[L] \to 0$. In our model, the sensitivity S can be readily determined analytically:

$$S \equiv -\frac{\partial \ln A_{wt}}{\partial \ln [L]}\Big|_{[L]=[L]_0} = N_a(1 - a_0)(1 - C) \times \frac{[L]_0/K}{(1 + C[L]_0/K)(1 + [L]_0/K)}. \quad (3)$$

The sensitivity reaches its maximum value S_{max} at background ligand concentration $[L]_0 = K/\sqrt{C}$, i.e., the geometrical mean of the two dissociation constants K and K/C, with S_{max} dependent on N_a, a_0, and C:

$$S_{max} = N_a(1 - a_0)\frac{1 - \sqrt{C}}{1 + \sqrt{C}}. \quad (4)$$

For a wide range of background MeAsp concentrations (2 μM to 5 mM), the sensitivity was calculated from experimental data $S \approx 4$. We can also estimate the value of $a_0 \approx \frac{1}{3}$ if we assume linear dependence of the FRET signal on the kinase activity for the full range of response in Sourjik and Berg (9). From Eq. 4, these lead to a lower bound for the number of Tar dimers in the functional complex $N_a \geq 6$ if we assume $C << 1$.

It is interesting to point out that within the MWC model, even though all the receptors (including Tar and Tsr) in the complex switch between the active and inactive states in an all-or-none fashion, the sensitivity to a specific type of stimulus only depend on the number of the corresponding receptors (that bind to the stimulus ligand) in the complex, as shown in Eq. 3 for the case of MeAsp response. This leads to the prediction that the sensitivity S could be larger for serine response (depending on the value of C for Tsr to serine) and should be much smaller for stimulus (such as galactose) that binds to the minor chemoreceptors (such as Trg) as compared to S for MeAsp.

Two scenarios for the wide dynamic range of high sensitivity

From Eq. 3, the sensitivity does not decrease significantly from its peak value as long as the background MeAsp concentration $[L]_0$ lies within the range between K and K/C. The wide dynamic range of high sensitivity can thus be achieved by having either a wide window spanned between K and K/C with small C and a fixed K, or a smaller but moving window with larger C and a variable K that increases with the background $[L]_0$ (or equivalently the receptor methylation level). In the following, we evaluate both of these possibilities quantitatively.

Scenario I: fixed value of K

In general, we obtain the model parameters by minimizing the error function defined as the average of the squared differences between all experimental data and model predictions. For the simple case considered here, the three parameters K, C, and N in our model can also be obtained directly from a few data points. Specifically, the added MeAsp concentration at half-maximum activity for zero ambient, $\Delta[L]_{\frac{1}{2}}$, defined by $A_{wt}(\Delta[L]_{\frac{1}{2}}, 0) = \frac{a_0}{2}$ is found to be $\Delta[L]_{1/2} \approx 2$ μM; for high background MeAsp concentration $[L]_0 = 5$ mM, the activity at $[L] > 10$ mM approaches roughly $\frac{a_0}{10}$. These two experimental data points, together with the measured sensitivity value ($S \sim 4$) and the estimate of the adapted activity $a_0 \approx \frac{1}{3}$, determine the model parameters: $N_a = 6$, $K = 18.2$ μM, $C = 0.006$.

Our model, with the above parameters determined by a small portion of the dose response data, should nonetheless describe all the response curves for wt cell in different MeAsp backgrounds. The response curves (*lines*) for ambient concentrations $[L]_0 = 0$, 100, 500, 5000 (μM) determined from our model are shown in Fig. 1 *A* together with experimental data (9) (*symbols*). The quantitative agreement between our model predictions and the experimental data provides strong justification for the model. The sensitivity $S = \frac{\Delta A_{wt}/a_0}{\Delta[L]/[L]_0}$ for $\Delta[L]/[L]_0 = 0.01$ is also calculated from our model for different background MeAsp concentrations as shown in Fig. 1 *B*. In this case (with fixed value of K), the wide range of high sensitivity is achieved by having a large value of $\frac{1}{C}$.

This simple case of MWC model with fixed value of K was also studied by Keymer et al. (18). However, their choice of parameters, in particular, the larger value of C ($C = 0.04$), leads to much less accurate agreement with the data, especially for higher MeAsp backgrounds. See Fig. 5 in Supplementary Material for other choices of parameters with less accurate fit to the data and the detailed comparison between the model behaviors for the parameter values from Keymer et al. (18) and the parameter values determined in this study.

Scenario II: variable K *and modest value of* $\frac{1}{C}$

For modest value of $\frac{1}{C}(<100)$, K needs to vary with background MeAsp concentration to explain the experimental data. For different values of C (>0.01), we fit the experimental data using our model with four different K's

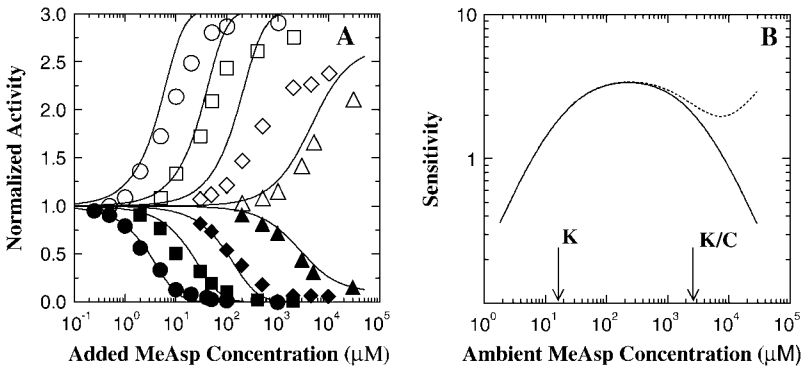

FIGURE 1 Kinase response and sensitivity for different MeAsp backgrounds. (*A*) The lines represent responses in kinase activity upon addition and removal of different concentrations of MeAsp, predicted by the adaptive allosteric model with constant value of $K = 18.2$ (μM), $C = 0.006$, and $N_a = 6$, for ambient MeAsp concentrations $[L]_0 = 0$, 100 μM, 500 μM, and 5 mM, together with the corresponding experimental results (*symbols*) taken from Sourjik and Berg (9). (*B*) The sensitivity value determined from the model for different ambient concentrations of MeAsp. The solid line is for a model without Tsr binding to MeAsp, and the dotted line is for a model with Tsr binding to MeAsp for high MeAsp concentrations, with $K_S = 50$ mM, $C_S = 0.1$. The contribution to the sensitivity from Tsr is apparent from the difference of the curves.

($K_I < K_{II} < K_{III} < K_{IV}$) for the four different backgrounds ($[L]_0 = 0$, 0.1, 0.5, 5 mM), respectively, and with N_a as a global fitting parameter. We find that there is a range of possible parameters with which our model can fit the experimental data with accuracy equal or better than the fit in scenario I. In Fig. 2, the possible values of the fold change in dissociation constants R_K ($\equiv K_{IV}/K_I$) and the corresponding total complex size $N = 3N_a$ (assuming Tsr is twice as abundant as Tar in wt cells) are represented by the lower and upper shaded regions, respectively. For an (arbitrary) set of parameters, $C = 0.1$, $N_a = 10$, $R_K \approx 6.7$, picked in the shaded regions in Fig. 2 (labeled by X), the dose response behaviors of our model (lines) are shown in the inset, in good agreement with the experimental data (symbols).

As shown in Fig. 2, for larger values of C, R_K, the variability in K, needs to be larger to extend the range of high sensitivity. The required complex size N also increases with C, as expected from Eq. 4, to maintain the magnitude of the sensitivity. In Fig. 2, the upper (lower) boundary for the allowed N ($= 3N_a$) values correspond to the lower (upper) boundary for the allowed R_K values. This means that cooperativity, measured by the complex size, also contributes to extend the high sensitivity range, because a smaller R_K is required to explain the experimental data with larger N_a. Taken together, the wide range of high sensitivity is maintained by the combination of small value of C, variability in K, and large value of complex size N_a.

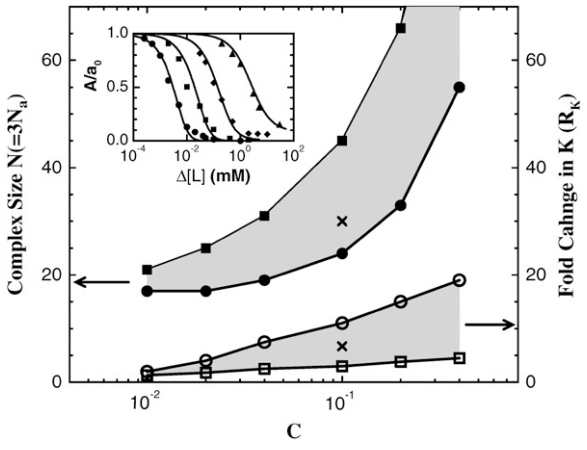

FIGURE 2 The values of allowed complex size $N = 3N_a$ (*upper shaded region*) and the corresponding values of affinity variation R_K (*lower shaded region*) for different values of $C \geq 0.01$ as determined by fitting the adaptive allosteric model to the response data of adding attractant from Sourjik and Berg (9). As C increases, the size of the required complex and the variation of dissociation constants increase. The effects of increasing N_a and R_K variation compensate each other, e.g., for a given C, the upper (*lower*) boundary of the complex size labeled by solid squares (*solid circles*) corresponds to the lower (*upper*) boundary for allowed R_K labeled by open squares (*open circles*). An arbitrary parameter set labeled by ''X'' in the allowed (*shaded*) parameter regions is picked with $C = 0.1$, $N_a = 10$, and $R_K = 6.7$ ($K_{I, II, III, IV} = 28.3, 31.2, 44.5, 189.7$ (μM)); the kinase activity determined from the adaptive allosteric model with these parameters is shown in the inset, together with experimental data (*symbols*).

So, which strategy (scenario) does *E. coli* use to maintain its wide dynamic range? From the wt response data alone, we cannot decide whether K depends on receptor methylation. Quantitative analysis of the in vitro kinase response measurements for Tar receptors in different methylation states carried out by Bornhorst and Falke (22) favors scenario II, i.e., what they called the heterogeneous two-state model (23). Our earlier modeling studies of the in vivo FRET measurements by using the Ising-type model (13,15) also show quantitative agreement with experimental data only with K dependent on receptor methylation level, though because of the complexity in solving the Ising-type model, we did not attempt to fit data for both wt cells and mutants with the same parameters. Recently, following the earlier work of Shimizu et al. (14), Keymer et al. (18) tried to use the MWC-type model to explain data from both the wt cells and several strains together with a constant value of K, i.e., scenario I; however, their modeling results show only qualitative agreements with the experimental data (for both wt cells and the mutant strains). Even though circumstantial evidence supports scenario II, at least for the in vivo system, more definitive experiments are needed to decide whether K depends on receptor methylation or not. In the Discussion section, we will suggest possible further in vivo response measurements in specific mutant strains that may distinguish these two scenarios unambiguously.

Adaptation tunes the system to the most sensitive part of the response curve

To best demonstrate the effects of adaptation, in Fig. 3 *A* we show the kinase response versus the full (final) MeAsp concentration $[L]$ (instead of the ligand concentration change $\Delta[L]$), which we call the full response curves, for different background MeAsp concentrations $[L]_0 = 0$, 0.03, 0.1, 0.2, 0.3, 0.5, 1, 2, 5, 10 mM using our model with parameters for scenario I. The adapted states, represented by open circles in Fig. 3 *A*, have the same kinase activity due to perfect adaptation to MeAsp. The lower and upper parts of a full response curve separated by the open circle represent the responses of the system to addition and removal of MeAsp from the same ambient MeAsp concentration. The available experimental data for $[L]_0 = 0$, 0.1, 0.5, 5 mM are shown as solid symbols in Fig. 3 *A*. The kinase response curves for the other MeAsp backgrounds ($[L]_0 = 0.03$, 0.2, 0.3, 1, 2, 10 mM) in Fig. 3 *A* represent quantitative predictions of our model. The full response curves show strong cooperativity with high Hill coefficient ($\sim$6) for the same range of ambient MeAsp concentrations where high sensitivity is observed. It can be shown that sensitivity as defined in Eq. 3 is linearly proportional to the Hill coefficient of the full response curve. Therefore, the full response curve, i.e., kinase activity versus the final ligand concentration $[L]$, is a better way to show the

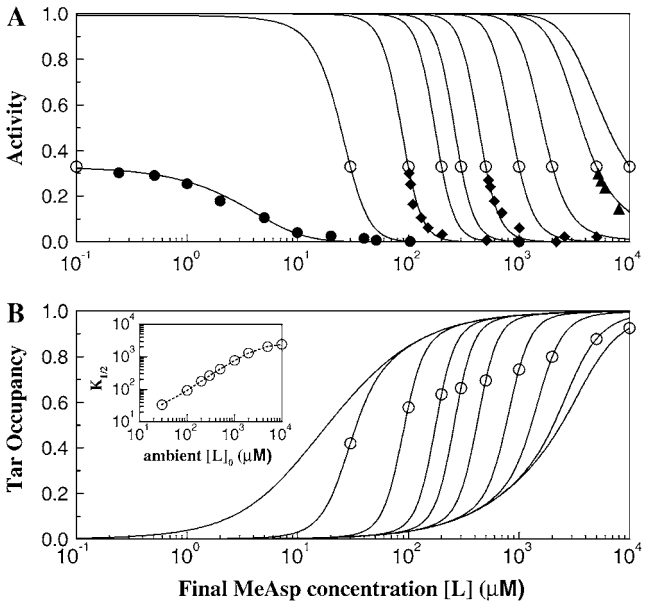

FIGURE 3 (*A*) The kinase activity and (*B*) the (instantaneous) Tar occupancy (fraction of Tar receptors bound to MeAsp), determined from the adaptive allosteric model, plotted versus the final MeAsp concentration. Different curves (from *left to right*) in both panels *A* and *B* correspond to wt cells adapted to different background MeAsp concentrations $[L]_0 = 0$, 0.03, 0.1, 0.2, 0.3, 0.5, 1, 2, 5, 10 mM. The open circles in both panels *A* and *B* represent the kinase activity and Tar occupancy in the adapted states. The available experimental kinase activity data for $[L]_0 = 0$, 0.1, 0.5, 5 mM are represented by solid circles, squares, diamonds, and triangles, respectively. The inset in panel *B* shows the dependence of the half-occupancy MeAsp concentration $K_{1/2}$ on the background MeAsp concentration $[L]_0$, to which the wt cells have adapted.

wt response data to reveal directly the cooperativity of the underlying system than is a plot of activity versus the ligand concentration change $\Delta[L]$ (as in Fig. 1 *A* here and in the original experimental article by Sourjik and Berg (9)), which shows a low Hill coefficient and conceals the true cooperativity of the system.

As the system adapts to higher background concentrations, the full response curve shifts to higher stimulus intensities driven by adaptation to keep a fixed level of activity for the adapted state, i.e., perfect adaptation. However, the more subtle but perhaps more important effect of adaptation is to keep the system at the most sensitive part of the response curves for a wide range of backgrounds as seen in Fig. 3 *A*. In other words, the cell optimizes its sensitivity indirectly by tuning the activity of the system to a certain level, which coincides with the most sensitive part of the response curves. This strategy of indirect sensitivity optimization is also found in other sensory systems (24).

The general understanding of the role of adaptation puts less stringent constraint on the accuracy of adaptation. As shown in Fig. 3 *A*, there is a finite range of kinase activities over which the response curve is steep and the cell has high sensitivity, therefore perfect accuracy of adaptation is not required to maintain the high sensitivity. This could partly explain the fact that *E. coli* responds to serine properly, even though the adaptation to serine is not perfect (21).

Receptor occupancy also adapts

For cells that have adapted to a background MeAsp concentration $[L]_0$, the immediate receptor occupancy upon sudden change of ligand concentration to a new value of $[L]$, $O([L], [L]_0)$, can be determined from our model: $O([L], [L]_0) = \frac{[L]}{[L]+K/C}A_{\mathrm{wt}} + \frac{[L]}{[L]+K}(1 - A_{\mathrm{wt}})$. In Fig. 3 *B*, we plot $O([L], [L]_0)$ vs. $[L]$ for different ambient MeAsp concentrations $[L]_0$ using parameters from scenario I (constant K), and the receptor occupancy for the adapted state, $O_{\mathrm{a}}([L]) \equiv O([L], [L])$, are shown as open circles. As a general consequence of adaptation in allosteric type models, $O_{\mathrm{a}}([L])$ shows a gradual (approximately logarithmic) dependence on the ligand concentration $[L]$, avoiding saturation until $[L] \gg K/C$. The receptor occupancy curves also shift with the ambient ligand concentration. In the inset of Fig. 3 *B*, the half-occupancy ligand concentration $K_{1/2}$, defined by $O(K_{1/2}, [L]_0) = \frac{1}{2}$, is plotted versus $[L]_0$; $K_{1/2}$ shows strong dependence (tracking) on $[L]_0$. An interesting consequence of this affinity tracking is the decrease in receptor occupancy caused by adaptation. Upon sudden increase of MeAsp concentration, the receptor occupancy goes up initially following one of the curves in Fig. 3 *B*; as the system adapts, the occupancy decreases, changing from the original curve to the one corresponding to the adapted state. Such adaptation in receptor occupancy should exist for a wide range of ambient ligand concentration. Another interesting quantity, defined as the ratio of the fractional change in activity to the fractional receptor occupancy change, was used in Sourjik and Berg (9) and given the name ''gain'' to relate kinase response directly with receptor occupancy. This gain is found to be in the range of 10–20 in our model (see supplemental Fig. 6 in Supplementary Material for details) depending on background MeAsp concentrations.

The qualitative behaviors in kinase activity and receptor occupancy affected by adaptation as shown in Fig. 3, *A* and *B*, are generic to the two-state allosteric models. Indeed, these general behaviors are also observed for our model with variable K (see supplemental Fig. 7 in Supplementary Material for details), with only quantitative differences.

Accurate adaptation maintains high Hill coefficient in population averaged response

In a single cell, there are many (decoupled) functional receptor complexes, with a distribution in their sizes and compositions due to intrinsic noise in the complex formation process. Therefore, even though a high Hill coefficient can be expected from individual receptor complex, an important

question remains as to whether summing the kinase activities over such heterogeneous population of complexes would destroy the cooperativity of the kinase response at the cell level. Indeed, if the locations of the most sensitive regimes of the individual complex had a wide distribution, the population averaged response curve would have a much reduced Hill coefficient. Fortunately, because the primary methylation and demethylation processes operate locally, i.e., between individual receptor dimer and its immediate neighboring dimers, accurate adaptation (through methylation/demethylation processes) is presumably maintained at the individual functional complex level. The accurate adaptation therefore effectively synchronizes the responses from different functional complexes by enforcing the same adapted activity for each individual complex, as demonstrated in Fig. 4 where each group of dotted lines, representing the kinase activities of different individual receptor complexes in a given MeAsp background, all pass through the same point with the same adapted kinase activity. As the result of this synchronization, the population averaged kinase response in a cell has the same high sensitivity as that of a single complex with the average number of Tar receptors, as demonstrated in Fig. 4 where kinase responses from individual complexes (*dotted lines*) and their averages (*thick solid lines*) are shown for different MeAsp backgrounds. This conclusion can also be reached analytically by averaging the sensitivity expressed in Eq. 3 over the population of different receptor complexes. If the accurate adaptation is only kept globally at the cellular level, different complexes could have different adapted activities, which would lead to reduced sensitivity. However, CheB phosphorylation, the only global component of the adaptation kinetics, is known to be irrelevant for perfect adaptation (25), making this global adaptation scenario less likely.

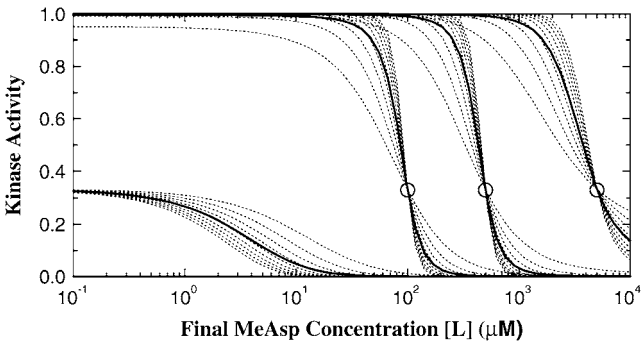

FIGURE 4 A population of receptor complexes is generated with the total number of receptor dimers (including Tar and Tsr) equally distributed between 17, 18, and 19, among which the number of Tar dimers is chosen from a binomial distribution with $p = 1/3$. The kinase responses for individual receptor complexes in the population are shown as dotted lines, determined from our model with the parameters, K and C, the same as in Fig. 1. The four groups of curves (from *left to right*) correspond to responses in four different ambient MeAsp backgrounds $[L]_0 = 0, 0.1, 0.5, 5$ mM. The responses from different receptor complexes are synchronized by their common adapted states represented by the open circles. The population averaged responses are shown as thick solid lines; they are almost indistinguishable from the responses of a single complex with the average number of Tar dimers ($N_a = 6$) shown in Fig. 3.

DISCUSSION

Additive sensitivity and the effect of methylation level distribution

For simplicity, we have assumed up to now that all the Tar receptors within a functional complex have the same methylation level, we now evaluate the effects of the methylation level distribution. Assume that each of the N Tar receptors in the functional complex has a different methylation level, and therefore different values of the dissociation constants, K_i and K_i/C_i (for the ith receptor in the functional complex). Following the generalized MWC model, the activity can now be written as:

$$A_{wt} = \frac{L\prod_{i=1}^{N}\left(1+\frac{C_i[L]}{K_i}\right)}{\prod_{i=1}^{N}\left(1+\frac{[L]}{K_i}\right)+L\prod_{i=1}^{N}\left(1+\frac{C_i[L]}{K_i}\right)}, \quad (5)$$

from which we can determine the sensitivity:

$$S \equiv -[L]\frac{\partial \ln A_{wt}}{\partial [L]}\Big|_{[L]=[L]_0} = (1-A_{wt})\sum_{i=1}^{N}\frac{(1-C_i)[L]_0/K_i}{(1+C_i[L]_0/K_i)(1+[L]_0/K_i)}. \quad (6)$$

This general result indicates that the contributions to the sensitivity from different receptors within the strongly coupled functional complex are additive, each receptor i in the complex ''contribute'' to the sensitivity S a term $\frac{(1-C_i)[L]_0/K_i}{(1+C_i[L]_0/K_i)(1+[L]_0/K_i)}$, which peaks when the ligand concentration $[L]_0$ falls into this particular receptor's most responsive regime $K_i < [L]_0 < K_i/C_i$. For the receptors that do not bind to the stimulus ligand, $K_i = \infty$, and there are no contributions to S from these receptors.

For response to MeAsp as considered in this article, the distribution of Tar methylation level only matters when K depends on receptor methylation level, i.e., in scenario II, where the methylation distribution leads to a distribution of K values. If the Tar methylation level distribution is not too broad and the most sensitive regimes (between K_i and K_i/C_i) for all the Tar receptors overlap strongly, our simplified analysis (neglecting methylation level distribution) should still be valid. If the distribution of methylation levels is so broad that only some of the Tar receptors contribute significantly to the sensitivity at a given $[L]_0$, then the large value of sensitivity has to be sustained by having larger values of N_a than those determined from our analysis in the

Results section for scenario II. Detailed analysis awaits further experimental data, such as direct measurements of receptor methylation distribution in cells adapted to different backgrounds. On the modeling side, Eq. 5 provides a concrete framework for relating detailed methylation configuration and dynamics to kinase activity in the wt cell, which is one of the remaining challenges in understanding bacterial chemotaxis for our future work.

The analysis on properties of mixed receptor complex leads naturally to possible experiments to distinguish the two scenarios considered in the Results section, i.e., to determine whether K depends on receptor methylation. We suggest measuring kinase activity in $CheR^{-}CheB^{-}Tsr^{-}$ mutant strains that contain only Tar receptor in a mixture of different methylation states (with most receptors in the QEQE or higher methylation states). If K is independent of methylation level (scenario I), the response curve for the mixed strain should be as steep as that of the same mutant strains but with Tar in a single methylation state (26). If K depends on receptor methylation level (scenario II), the response curve would be less steep, and the decrease in steepness depends on the amount of variation in K (for all the receptors in the complex) as compared to the parameter C, as shown in Eq. 5.

The effect of Tsr binding to MeAsp at high MeAsp concentration

The above general analysis also helps us understand the effects of Tsr with respect to response to MeAsp. Tsr can bind to MeAsp, but at a much higher MeAsp concentration. Within the normal range of background MeAsp concentrations (< 5 mM), i.e., for all of the wt response data considered in this article, the Tsr receptors are mostly unbound and they affect the sensitivity of the system only through their contributions to the overall equilibrium constant L of the functional complex. That is why we can get good fit to the data without considering MeAsp Tsr binding. We tried to fit the data with Tsr MeAsp binding explicitly included in our model; as expected, the quality of the fit does not seem to improve significantly (see supplemental Fig. 5 *B* in Supplementary Material for details). However, as the MeAsp concentration increases into the region within Tsr/MeAsp binding affinity, the contribution from the Tsr receptors becomes significant, and indeed dominates the overall sensitivity to MeAsp when $[L]_0$ is outside the Tar responsive regime. This shift of dominant contribution to S from Tar to Tsr could help extend the range of high sensitivity. In Fig. 1 *B*, we show the sensitivity curve (*dotted line*) once we include the Tsr binding to MeAsp with $K_S = 50$ (mM) and $C_S = 0.1$ in our model (the parameters for Tar are taken from scenario I). The sustained high sensitivity beyond 5 mM is due to the direct contribution from Tsr. The second peak in the sensitivity curve due to the Tsr contribution was also seen in experiment, as shown in Fig. 3 *B* in Sourjik and Berg (9).

The removal of attractants

In Fig. 1 *A*, the responses for removal of MeAsp (*upper curves*) are plotted from our model with parameters in scenario I, showing qualitative agreement with experimental data. Quantitatively, the removal curves for the intermediate ambient concentrations, $[L]_0 = 100, 500$ (μM), do not reach the maximum activity in the experiments, in contrast to the model behaviors. We do not understand this discrepancy yet. However, we need to point out that due to the way the experiments in Sourjik and Berg (9) were set up, different points on each removal curve in Fig. 1 *A* represent responses from different adapted states. New removal experiments from a fixed adapted state, i.e., from a constant ambient concentration $[L]_0$ to $[L]_0 - \Delta[L]$, consistent with the way experiments of the addition of MeAsp were carried out, will be more informative.

Possible complex size dependence on receptor methylation level can also be evaluated using our model. As background ligand concentration $[L]_0$ increases beyond K/C, the contribution to sensitivity from each individual receptor decreases significantly, however, as is evident from Eq. 3, an increase in the number of receptors in the complex, N can maintain the overall sensitivity of the complex. If N increases with $[L]_0$ or receptor methylation level, the requirement on C can be less stringent to maintain the wide range of high sensitivity. For example, good agreement with experimental data can be achieved for $C = 0.1$ for a constant K if N can increase approximately sixfold as the cell adapts to 5 mM of MeAsp (see text and Figs. 8 and 9 in Supplementary Material).

SUMMARY

From our analysis in this article, a comprehensive understanding of the high sensitivity and its wide dynamic range in bacterial chemotaxis has emerged. First, we find that the heightened sensitivity is a direct consequence of receptor cooperativity. In particular, the sensitivity to a given ligand is amplified linearly by the number of corresponding receptors in the highly cooperative functional complex. Second, we find that adaptation, through directly controlling the kinase activity, effectively tunes the system to the steepest part of the response curves. In addition, adaptation synchronizes the responses from different receptor complexes within a single cell so that the averaged response of the cell (over many individual receptor complexes) remains highly cooperative (with a high Hill coefficient).

The dynamic range of the high sensitivity is determined by the range of possible dissociation constants K for the receptor in its different conformational (active and inactive) and

covalent modification (methylation) states. For the simple case where K is independent of receptor methylation, properties of the complex and the receptor can be determined: $N_a = 6$, $K = 18.2\ \mu$M, and $C = 0.006$, where the small value of C is required to maintain high sensitivity over three orders of magnitude of background MeAsp concentrations. For larger values of C, K and/or N need to increase with receptor methylation level for our model to explain the experimental data. For example, with $C = 0.1$, K needs to change approximately sevenfold to account for the range of high sensitivity if we assume the complex contains ~10 Tar receptor dimers; another possibility is for the number of receptors in the complex to increase by approximately sixfold while keeping K constant. The currently available response data for wt cells are consistent with all these different scenarios. The in vitro kinase response measurements (22,23) and our earlier modeling studies using the Ising-type model (13,15) favor the scenario with K dependent on receptor methylation level. Future in vivo kinase activity measurements for cells with Tar receptors in (controlled) mixed methylation states could help us unambiguously distinguish these different scenarios. The situation may be quantitatively different for receptor Tsr in response to serine, where in vitro ligand binding measurements show very small dependence on Tsr methylation level. Although the in vitro experimental data for both ligand binding and kinase activity measured in Levit and Stock (27) can be explained together by a MWC model with a constant K and a large value of $C \approx 0.5$, more works are needed to understand the apparent differences between in vitro kinase activity measurements from different groups (27,28).

In response to a sudden increase in ligand concentration, the receptor occupancy will increase initially. However, as a general consequence of the adaptive allosteric model, the receptor occupancy should subsequently decrease as the cell adapts. Such receptor occupancy adaptation, which may not be as accurate as the adaptation in kinase activity, should exist for a wide range of ambient ligand concentrations. As a result of this receptor occupancy adaptation, the receptor occupancy in the adapted cell should have more gradual (approximately logarithmic) dependence on the background ligand concentration than the binding curve with a fixed dissociation constant, prolonging high sensitivity by avoiding receptor saturation. An earlier in vitro experiment (29) detected a modest dependence of ligand binding on methylation (6–10-fold change in k_d between *EEEE* and *QEmQEm* or *EmEmEmEm*) for (isolated) Tar receptors without CheW and CheA. It will be more informative to carry out the ligand binding experiments for Tar in the signaling complex (with CheW and CheA), and measure kinase activity simultaneously as done in Levit and Stock (27) for Tsr. Ultimately, to unambiguously test the validity of the general allosteric type model for bacterial chemotaxis and to determine whether and by how much K and N depend on receptor methylation level, it may be necessary to measure receptor occupancy in wt cells as they respond to various stimuli in different backgrounds.

SUPPLEMENTARY MATERIAL

An online supplement to this article can be found by visiting BJ Online at http://www.biophysj.org.

We thank Dr. Howard Berg and Dr. Victor Sourjik for explaining their experiments to us. We thank Dr. Geoff Grinstein for careful reading of the manuscript.

REFERENCES

1. Koshland, D. E., A. Goldbeter, and J. B. Stock. 1982. Amplification and adaptation in regulatory and sensory systems. *Science*. 217:220–225.
2. Torre, V., J. F. Ashmore, T. D. Lamb, and A. Menini. 1995. Transduction and adaptation in sensory receptor cells. *J. Neurosci.* 15:7757–7768.
3. Bren, A., and M. Eisenbach. 2000. How signals are heard during bacterial chemotaxis: protein-protein interactions in sensory signal propagation. *J. Bacteriol.* 182:6865–6873.
4. Falke, J. J., and G. Hazelbauer. 2001. Transmembrane signaling in bacterial chemoreceptors. *Trends Biochem. Sci.* 26:257–265.
5. Maddock, J. R., and L. Shapiro. 1993. Polar location of the chemoreceptor complex in the *E. coli* cell. *Science*. 259:1717–1723.
6. Bray, D., M. D. Levin, and C. J. Morton-Firth. 1998. Receptors clustering as a cellular mechanism to control sensibility. *Nature*. 393:85–88.
7. Duke, T. A. J., and D. Bray. 1999. Heightened sensitivity of a lattice of membrane of receptors. *Proc. Natl. Acad. Sci. USA*. 96:10104–10108.
8. Shi, Y. 2000. Adaptative Ising model and bacterial chemotatic receptor network. *Europhys. Lett.* 50:113–119.
9. Sourjik, V., and H. C. Berg. 2002. Receptors sensitivity in bacterial chemotaxis. *Proc. Natl. Acad. Sci. USA*. 99:123–127.
10. Sourjik, V. 2004. Receptor clustering and signal processing in *E. coli* chemotaxis. *Trends Microbiol.* 12:569–576.
11. Segall, J. E., S. M. Block, and H. C. Berg. 1983. Temporal comparisons in bacterial chemotaxis. *Proc. Natl. Acad. Sci. USA*. 31:8987–8991.
12. Sourjik, V., and H. C. Berg. 2004. Functional interactions between receptors in bacterial chemotaxis. *Nature*. 428:437–441.
13. Mello, B. A., and Y. Tu. 2003. Quantitative modeling of sensitivity in bacterial chemotaxis: the role of coupling among different chemoreceptor species. *Proc. Natl. Acad. Sci. USA*. 100:8223–8228.
14. Shimizu, T. S., S. V. Aksenov, and D. Bray. 2003. A spatially extended stochastic model of the bacterial chemotaxis signalling pathway. *J. Mol. Biol.* 329:291–309.
15. Mello, B. A., L. Shaw, and Y. Tu. 2004. Effects of receptor coupling in bacterial chemotaxis. *Biophys. J.* 87:1578–1595.
16. Rao, C. V., M. Frenklach, and A. P. Arkin. 2004. An allosteric model for transmembrane signaling in bacterial chemotaxis. *J. Mol. Biol.* 343:291–303.
17. Mello, B. A., and Y. Tu. 2005. An allosteric model for heterogeneous receptor complexes: understanding bacterial chemotaxis response to multiple stimuli. *Proc. Natl. Acad. Sci. USA*. 102:17354–17359.
18. Keymer, J. E., R. G. Endres, M. Skoge, Y. Meir, and N. S. Wingreen. 2006. Chemosensing in *E. coli*: two regimes in two-state receptors. *Proc. Natl. Acad. Sci. USA*. 103:1786–1791.
19. Monod, J., J. Wyman, and J. P. Changeux. 1965. On the nature of allosteric transitions: a plausible model. *J. Mol. Biol.* 12:88–118.

20. Sokge, M. L., R. G. Endres, and N. S. Wingreen. 2006. Receptor-receptor coupling in bacterial chemotaxis: evidence for strongly coupled clusters. *Biophys. J.* 90:4317–4326.

21. Berg, H. C., and D. A. Brown. 1972. Chemotaxis in *Escherichia coli* analysed by three dimensional tracking. *Nature.* 239:500–504.

22. Bornhorst, J. A., and J. J. Falke. 2001. Evidence that both ligand binding and covalent adaptation drive a two-state equilibrium in the aspartate receptors signaling complex. *J. Gen. Physiol.* 118: 693–710.

23. Bornhorst, J. A., and J. J. Falke. 2003. Quantitative analysis of aspartate receptor signaling complex reveals that the homogeneous two-state model is inadequate: development of a heterogeneous two-state model. *J. Mol. Biol.* 326:1597–1614.

24. Laughlin, S. 1989. The role of sensory adaptation in the retina. *J. Exp. Biol.* 146:39–62.

25. Alon, U., M. G. Surette, N. Barkai, and S. Leibler. 1999. Robustness in bacterial chemotaxis. *Nature.* 397:168–171.

26. Shimizu, T. S., N. Delalez, K. Pichler, and H. Berg. 2006. Monitoring bacterial chemotaxis by bio-luminescence resonance energy transfer: absence of feedback from the flagellar motor. *Proc. Natl. Acad. Sci. USA.* 103:2093–2097.

27. Levit, M. N., and J. B. Stock. 2002. Receptor methylation controls the magnitude of stimulus-response coupling in bacterial chemotaxis. *J. Biol. Chem.* 277:36760–36765.

28. Li, G., and R. M. Weis. 2000. Covalent modification regulates ligand binding to receptor complexes in the chemosensory system of *Escherichia coli*. *Cell.* 100:357–365.

29. Borkovich, K. A., L. A. Alex, and M. I. Simon. 1992. Attenuation of sensory receptor signaling by covalent modification. *Proc. Natl. Acad. Sci. USA.* 89:6756–6760.